

PWM inverter-excited iron loss characteristics of a reactor core

Atsushi Yao, Kouhei Tsukada, Shunya Odawara, Keisuke Fujisaki, Yuji Shindo, Naoki Yoshikawa, and Tetsuma Yoshitake

Citation: *AIP Advances* **7**, 056618 (2017); doi: 10.1063/1.4973797

View online: <http://dx.doi.org/10.1063/1.4973797>

View Table of Contents: <http://aip.scitation.org/toc/adv/7/5>

Published by the [American Institute of Physics](#)

Articles you may be interested in

[Large magnetoresistance effect in nitrogen-doped silicon](#)

AIP Advances **7**, 056604056604 (2016); 10.1063/1.4972795

[Effect of partial saturation of bonded neo magnet on the automotive accessory motor](#)

AIP Advances **7**, 056611056611 (2016); 10.1063/1.4973496

[Measurement of rotational magnetic properties of nanocrystalline alloys by a modified B-H sensor](#)

AIP Advances **7**, 056614056614 (2016); 10.1063/1.4973595

[The first-principles investigations on magnetic ground-state in Sm-doped phenanthrene](#)

AIP Advances **7**, 055704055704 (2017); 10.1063/1.4973746

HAVE YOU HEARD?

Employers hiring scientists and
engineers trust

PHYSICS TODAY | JOBS

www.physicstoday.org/jobs



PWM inverter-excited iron loss characteristics of a reactor core

Atsushi Yao,^{1,a} Kouhei Tsukada,¹ Shunya Odawara,¹ Keisuke Fujisaki,¹
Yuji Shindo,² Naoki Yoshikawa,² and Tetsuma Yoshitake²

¹Toyota Technological Institute, Nagoya 468-8511, Japan

²Kawasaki Heavy Industries Ltd., Akashi 673-8666, Japan

(Presented 2 November 2016; received 23 September 2016; accepted 20 October 2016;
published online 4 January 2017)

In this paper, we focus on an evaluation of iron losses in a reactor core under pulse width modulation (PWM) inverter excitation. We examine the inverter- and sinusoidal-fed iron losses of the reactor core through both experiments and numerical simulations. The proposed measurement includes operation at a higher frequency than is used commercially. We discuss the building factor (BF) of reactor losses under PWM inverter and sinusoidal excitations based on material iron losses measured in a ring specimen. The BF calculation based on inverter-fed tests is an almost constant value because the magnetic flux density distributions related to the carrier frequency mostly do not depend on the reactor gaps. © 2017 Author(s). All article content, except where otherwise noted, is licensed under a Creative Commons Attribution (CC BY) license (<http://creativecommons.org/licenses/by/4.0/>). [<http://dx.doi.org/10.1063/1.4973797>]

I. INTRODUCTION

Reactors are made mostly of silicon steel and are widely used as filters in pulse width modulation (PWM) inverter circuits to reduce the harmonic component or in boost converters to store the electrical energy instantaneously. It is known that an iron core made of silicon steel has magnetic properties that are very different whether it is fed by sinusoidal or inverter voltages.¹⁻⁴ Therefore, in order to estimate the iron losses of an iron core under the PWM inverter excitation with sufficient accuracy, it is necessary to correctly understand the influence of carrier frequency.

Recently, reactor and inductor losses have been evaluated under sinusoidal excitation,^{5,6} square-formed excitation,⁷ and an AC filter.^{8,9} It is important to evaluate the impact of reactor core losses. In this study, the iron loss characteristics of an inverter-excited reactor are evaluated and compared to the case of sinusoidal-fed operation.

The building factor (BF) of any magnetic core is defined as the ratio between the losses of the iron core and the iron losses of the material. The evaluation of BF allows us to understand the iron losses caused by factors such as the manufacturing process, the core geometrical configuration, or any effects of the operating conditions not related to the material itself. Some studies have focused on the building factors evaluated in transformers,¹⁰ reactors under sinusoidal excitation,⁶ and motors.^{11,12} The next step is to understand the iron losses under PWM inverter excitation using the BF.

This paper addresses the evaluation of iron losses of a reactor core under PWM inverter excitation. We examine inverter- and sinusoidal-fed iron losses of a reactor core through both experiments and numerical simulations. The proposed measurement includes higher frequency operation than the commercial one. Furthermore, we discuss the BF of reactor losses under PWM inverter and sinusoidal excitations based on material iron losses measured in a ring specimen.

^aElectronic mail: yao@toyota-ti.ac.jp

II. EXPERIMENT AND NUMERICAL METHOD

A. Experimental setup of reactor and ring tests

Figure 1 illustrates the configuration of the experimental setup used to measure the iron loss characteristics of the reactor core (CS-125)^{6,13} made of non-oriented (NO) electrical steel sheets (35H300). An air gap of the reactor core is set at 2 mm, the core mass M_{rea} is 1.4 kg, and the number of turns of the reactor coil is 320.

Here, we perform two kinds of reactor iron loss tests. The first reactor test consists of exciting the core with a sinusoidal voltage using a function generator and a linear amplifier. The second test is to measure the iron loss of the reactor core excited by a single-phase PWM inverter. In this manner, the iron losses of the reactor core are affected by the PWM carrier frequency, unlike the first test. The PWM inverter output has a fundamental frequency f_0 and a carrier frequency f_c . In the following experiments, the modulation index m is set to 0.5 and the switching dead time is set to 3500 ns.

We now discuss the estimation method for obtaining the reactor iron losses under inverter and sinusoidal excitations. The reactor input active electrical power P_{in} is measured by an analog-to-digital (A/D) converter (PXI-5122, National Instruments). The measurement sampling frequency is 10 MHz and the resolution is 14 bit. In order to calculate the copper losses, the rms current I_1 is calculated from the obtained current waveform. The reactor iron loss can be obtained as

$$W_{\text{rea}} = P_{\text{in}} - I_1^2 R, \quad (1)$$

where $R(=0.56 \Omega)$ denotes the resistance of four coils in series.

In our experiments, the magnetic flux density B_{rea} is measured using a B -coil wound around the reactor core and is given by $B_{\text{rea}} = \int V_{\text{rea}} dt / (N_{\text{rea}} S_{\text{rea}})$, where V_{rea} denotes the B -coil voltage, $N_{\text{rea}} (=5)$ is the number of turns of B -coils, and $S_{\text{rea}} (=665 \text{ mm}^2)$ is the cross-sectional area of the reactor core. The peak magnetic flux density in the reactor is adjusted by tuning the applied voltage.

In this paper, in order to obtain the BF, we also perform measurements of the iron losses of the ring specimen under inverter and sinusoidal excitations as shown in Fig. 1. The ring specimen is made of NO electrical steel sheets using a wire-cut technique to reduce the deterioration of magnetic properties by mechanical stress. In our study, the iron loss of the ring specimen is regarded as the material loss. The iron loss based on the ring core can be described by

$$W_{\text{ring}} = M_{\text{rea}} \frac{f_0}{\phi} \int H dB, \quad (2)$$

where $\phi (=7650 \text{ kg/m}^3)$ is the density of the magnetic sheet, $H = N_1 I / L$ is the magnetic field intensity, and $B = \int V dt / (N_2 S)$ is the magnetic flux density. Here I is the input current, $N_1 (=254)$ is the number of turns of the exciting coil, $L (=0.36 \text{ m})$ is the average magnetic path length, V is the B -coil voltage, $N_2 (=254)$ is the number of turns of B -coils, and $S (=87.5 \text{ mm}^2)$ is the cross-sectional area of the ring. In the same manner as in the reactor test, the applied voltage is adjusted to obtain the required magnetic flux density (See Ref.2 for details of the ring measurements).

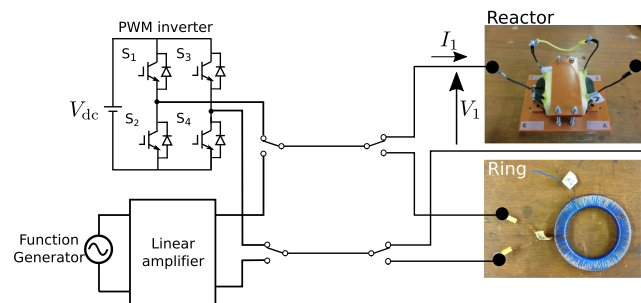


FIG. 1. Schematic of reactor and ring tests to experimentally measure the iron losses. We considered two excitation methods: PWM inverter and sinusoidal excitations.

We discuss the method of evaluating the BF of the reactor core. To do this, we proposed a comparison of the iron loss of the ring core W_{ring} with the iron loss of the reactor core W_{rea} . That is, the BF is described by

$$BF = \frac{W_{\text{rea}}}{W_{\text{ring}}}. \quad (3)$$

Note that, for the calculation, W_{ring} can be either $W_{\text{ring sin}}$ or $W_{\text{ring inv}}$ depending on whether the sinusoidal-fed ring test or the inverter-fed ring test is being considered.

B. Numerical method

Figure 2 shows an analysis model for the finite-element method (FEM) with $A - \phi$ method. The laminating structure is homogenized as a bulk structure in the model. The total iron losses of the reactor and ring specimen correspond to the hysteresis and eddy current losses. The experimental trials give the total reactor iron losses but not the loss repartition between the hysteresis loss and eddy-current loss in the laminating, rolling, and transverse directions. To discuss the loss repartition and characteristics, we perform a finite element analysis. Based on the experimental parameters, ideal voltage waveforms are used as the input of the numerical analysis, which is a time-stepped simulation.

In our numerical simulation, the iron losses of the reactor core W_{reanum} are described by

$$W_{\text{reanum}} = W_{\text{hys}} + W_{\text{eddy lami}} + W_{\text{eddy tran and rol}}, \quad (4)$$

$$W_{\text{hys}} = \sum_{ie=1}^{ne} \left[\sum_{k=1}^N \{ \alpha_{\text{roll}}(|B_{\text{roll},k}|)f_k + \alpha_{\text{tran}}(|B_{\text{tran},k}|)f_k + \alpha_{\text{lami}}(|B_{\text{lami},k}|)f_k \} \right] v_{ie}, \quad (5)$$

$$W_{\text{eddy tran and rol}} = \frac{\kappa}{T} \sum_{t=1}^{\text{step}} \frac{1}{v_{\text{(total)}}} \sum_{ie=1}^{ne} \frac{J^2(t)_{(ie)}}{\sigma_{(ie)}} v_{ie} \Delta t, \quad (6)$$

$$W_{\text{eddy lami}} = \sum_{ie=1}^{ne} \sum_{k=1}^N \beta_{\text{lami}}(|B_{\text{lami},k}|, f_k) f_k^2 v_{ie}, \quad (7)$$

where W_{hys} denotes the hysteresis loss, $W_{\text{eddy lami}}$ is the eddy current loss in the laminating direction, and $W_{\text{eddy tran and rol}}$ is the eddy current loss in the transverse and rolling directions. Here, α is the coefficient of hysteresis loss, $\kappa (= 2)$ is the anomaly factor, β is the coefficient of eddy current loss, B is the magnetic flux density, f is the frequency, T is the period, σ is the conductivity, v is the volume, and $ne (= 215, 200)$ is the number of elements. Finally, ie represents the element number. Here, the conductivities in the laminating, rolling, and transverse directions are set at 0 S/m, 1.923×10^6 S/m, and 1.923×10^6 S/m, respectively.

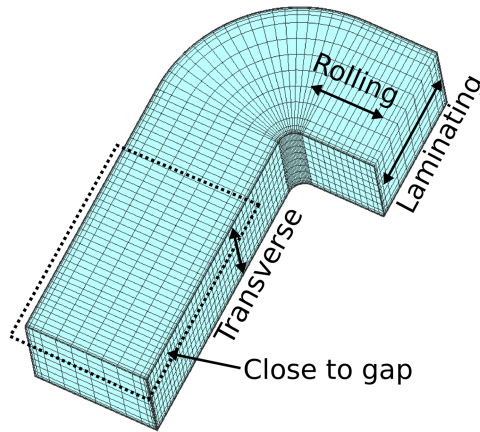


FIG. 2. Schematic of numerical model (1/8-region model). The working conditions based on the experimental results are simulated by three-dimensional (3D) FEM using the JMAG software. See Ref.5 for the details of the 3D FEM model.

III. RESULTS AND DISCUSSION

A. Experimental results and discussion

Figure 3 (a) shows the reactor loss characteristics with respect to the carrier frequency at ($f_0 = 50$ Hz; $B = 0.6$ T) and ($f_0 = 500$ Hz; $B = 0.1$ T). The iron losses of reactor core for these two parameters have the same tendency. The iron losses under inverter excitation decrease with increasing carrier frequency. The figure also shows the reactor iron loss under sinusoidal excitation for comparison purposes. The reactor core losses increase compared with the sinusoidal-fed operation because of $B-H$ curve minor loops² and increasing eddy currents.

Figure 3 (b) shows the ring loss characteristic as a function of the carrier frequency. The experimental ring tests are done in the same manner as the reactor tests. The iron losses in the inverter-fed ring show the same tendency as in the reactor core under inverter excitation, as shown in Fig. 3 (a). The reactor losses are larger than those of the material due to the increasing eddy current losses caused by the leakage magnetic flux density near the reactor gaps.

Figure 3 (c) shows the BF calculation results for each of the tested carrier frequencies at ($f_0 = 50$ Hz; $B = 0.6$ T) and ($f_0 = 500$ Hz; $B = 0.1$ T). As mentioned above, the BF differs with the type of ring test, which corresponds to iron losses under inverter and sinusoidal excitations ($W_{ringinv}$ and $W_{ringsin}$). Because the iron losses in the inverter-fed ring test are larger than those in the sine-fed ring test, the BF calculated based on the sine-fed test is larger. The iron losses of the reactor under inverter excitation are logically higher than the intrinsic material iron loss.

The BF calculated based on the inverter-fed test is almost a constant value as shown by the red lines in Fig. 3 (c) at ($f_0 = 50$ Hz; $B = 0.6$ T) and ($f_0 = 500$ Hz; $B = 0.1$ T). Note that the eddy currents at the end of the reactor core increase locally due to fringing flux caused by the air gap. However, for material and reactor iron losses under inverter excitation, the rate of decrease of iron losses as a function of the carrier frequency is almost the same value. In the next section, the reason for having the almost constant value is discussed using numerical simulations.

B. Numerical results and discussion

Here, we investigate the iron loss repartition and characteristics using 3D-FEM. Due to the high frequency of the carrier signal, it is necessary to have a high sampling frequency for the data input in the numerical simulations. This means a small time step and then a long calculation time. To reduce the calculation time, only the cases at $f_c = 1$ and 4 kHz under inverter excitation are simulated at $f_0 = 50$ Hz.

Figure 4 (a) shows the reactor iron losses under sinusoidal excitation and inverter excitation at $f_c = 1$ and 4 kHz. Here, the calculated total iron losses are about 0.85 W lower than the measurement at $f_c = 1$ kHz in Fig. 3 (a). However, the numerically obtained results in Fig. 4 (a) are qualitatively in agreement with the experimental results in Fig. 3 (a). Thus, based on the numerical and experimental results, we can qualitatively discuss the iron loss with respect to the carrier frequency.

As shown in Fig. 4 (a), $W_{eddy\text{lami}}$ accounts for about 30% and 21% of the total iron losses at $f_c = 1$ and 4 kHz, respectively. $W_{eddy\text{lami}}$ decreases with increasing carrier frequency. However, when f_c is changed, $W_{eddy\text{tranandrol}}$ and W_{hys} are almost the same. The rate of decrease of total iron losses as a function of the carrier frequency is caused by the eddy current loss in the laminating direction.

Figures 4 (b) and (c) show the magnetic flux density distributions for calculating $W_{eddy\text{lami}}$ on the area indicated by the square in Fig. 2. These figures show the distributions normalized by each maximum value of magnetic flux densities at 1.95 and 7.95 kHz, which correspond to about twice the respective carrier frequencies ($f_c = 1$ and 4 kHz). Here, the eddy current losses at 1.95 and 7.95 kHz correspond to each maximum value in harmonic components with the carrier frequency. When f_c is set at 1 kHz as shown in Fig. 4 (b), the strong region of the magnetic flux density (green region) expands compared to $f_c = 4$ kHz in Fig. 4 (c). Thus, $W_{eddy\text{lami}}$ increases with decreasing carrier frequency. Note also that, in the magnetic flux density distributions, the region close to the reactor gap and other regions of the reactor show almost the same characteristics. It is believed that the rate

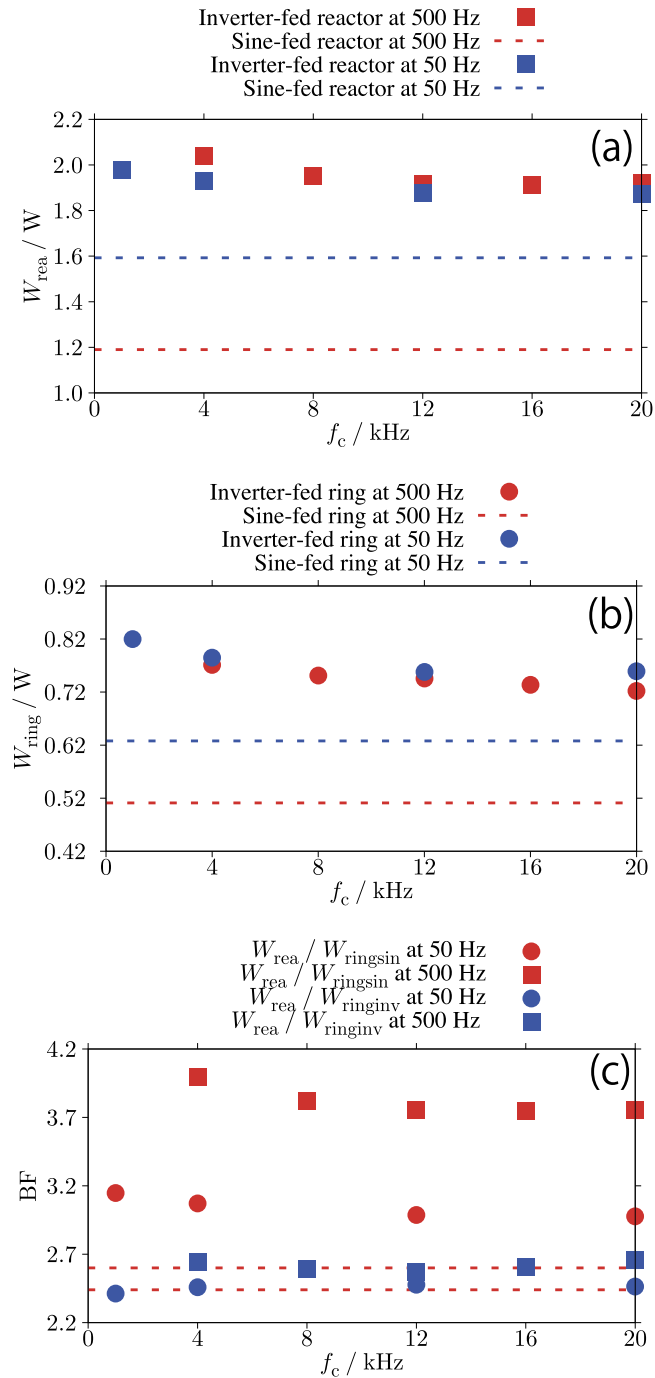


FIG. 3. Experimentally obtained reactor core losses, ring iron losses, and BF as a function of carrier frequency. Tests are done at carrier frequencies of 1, 4, 12, and 20 kHz (4, 8, 12, 16, and 20 kHz) at $f_0 = 50$ Hz and $B = 0.6$ T ($f_0 = 500$ Hz and $B = 0.1$ T). (a) Reactor core losses obtained from Eq. (1); (b) Ring losses from Eq. (2); (c) BF obtained from Eq. (3). When the inverter-fed (sine-fed) ring test is considered, the BF values versus f_c are represented by blue (red) dots.

of decrease as a function of the carrier frequency has the same tendency between the reactor and ring tests. Therefore, the BF calculated based on the inverter-fed test is an almost constant value and it is expected that we can estimate the iron losses of the reactor based on those of the ring test. Further numerical and experimental studies are necessary to realize a loss estimation method based on the BF.

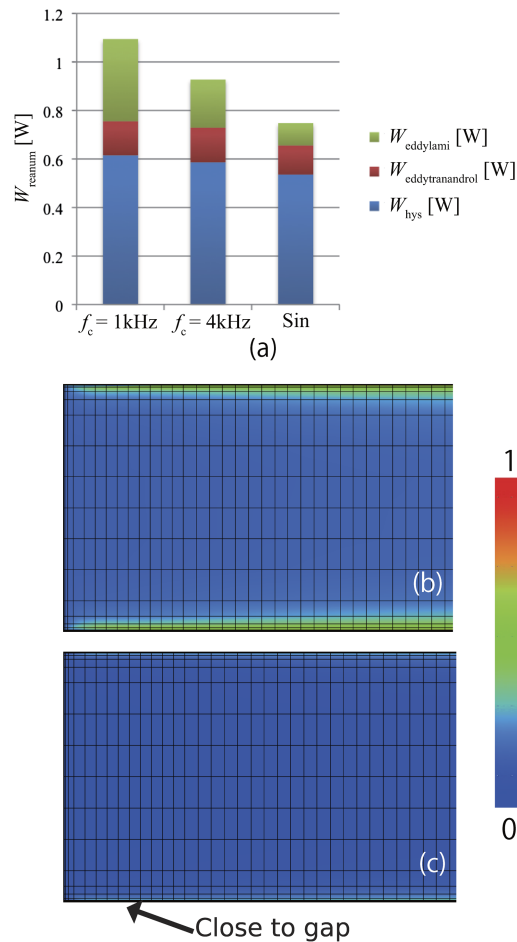


FIG. 4. Numerically obtained iron loss repartition and magnetic flux density distributions at $f_0 = 50\text{ Hz}$; (a) Iron loss repartition obtained from Eqs. (4), (5), (6) and (7); (b) Magnetic flux density distribution for calculating W_{eddydami} with Eq. (7) at 1.95 kHz and $f_c = 1\text{ kHz}$ in the square area of Fig. 2. The magnetic flux density distribution is normalized by its maximum value. At 1.95 kHz, W_{eddydami} depending on $f_c = 1\text{ kHz}$ becomes the maximum value; (c) Magnetic flux density distribution at 7.95 kHz and $f_c = 4\text{ kHz}$ using the same method as shown in (b).

IV. CONCLUSION

We focused on the impact of reactor core losses under PWM inverter and sinusoidal excitations. We experimentally and numerically confirmed that the iron losses of the reactor core decrease with increasing carrier frequency. To discuss the iron loss characteristics of the reactor core and BF, a comparison with the material iron loss was also performed under inverter and sinusoidal excitations. The inverter-fed ring showed the same tendency as the reactor core under inverter excitation at fundamental frequencies of 50 and 500 Hz. The BF calculated based on the inverter-fed test was an almost constant value because the magnetic flux density distributions related to the carrier frequency mostly did not depend on the reactor gaps. It is expected that we can estimate the iron losses of the reactor based on those of the ring test. The evaluation of the BF of reactor iron losses excited by an inverter using commercial and higher frequencies will be keys to designing the reactor core.

¹ M. Kawabe, T. Nomiya, A. Shiozaki, H. Kaihara, N. Takahashi, and M. Nakano, *IEEE Transactions on Magnetics* **48**, 3458 (2012).

² K. Fujisaki and S. Liu, *Journal of Applied Physics* **115**, 17A321 (2014).

³ S. Odawara, K. Fujisaki, and F. Ikeda, *IEEE Transactions on Magnetics* **50**, 1 (2014).

⁴ T. Taitoda, Y. Takahashi, and K. Fujiwara, *IEEE Transactions on Magnetics* **51**, 1 (2015).

⁵ S. Odawara, S. Yamamoto, K. Sawatari, K. Fujisaki, Y. Shindo, N. Yoshikawa, and T. Konishi, *IEEE Transactions on Magnetics* **51**, 1 (2015).

- ⁶ S. Odawara, N. Denis, S. Yamamoto, K. Sawatari, K. Fujisaki, Y. Shindo, N. Yoshikawa, and T. Konishi, [IEEE Transactions on Magnetics](#) **51**, 1 (2015).
- ⁷ N. Kurita, K. Onda, K. Nakanoue, and K. Inagaki, [IEEE Transactions on Power Electronics](#) **29**, 3657 (2014).
- ⁸ T. Shimizu and S. Iyasu, [IEEE transactions on Industrial Electronics](#) **56**, 2600 (2009).
- ⁹ H. Matsumori, T. Shimizu, K. Takano, and H. Ishii, [IEEE Transactions on Power Electronics](#) **31**, 3080 (2016).
- ¹⁰ H. Pfützner, G. Shilyashki, P. Hamberger, M. Aigner, F. Hofbauer, M. Palkovits, G. Trenner, E. Gerstbauer, I. Matkovic, and V. Galabov, [IEEE Transactions on Magnetics](#) **50**, 1 (2014).
- ¹¹ A. Boglietti, in Industry Applications Conference, 1999. Thirty-Fourth IAS Annual Meeting. Conference Record of the 1999 IEEE (IEEE, 1999), Vol. 1, pp. 489–493.
- ¹² N. Denis, S. Odawara, and K. Fujisaki, [IEEE Transactions on Industrial Electronics](#) (2016) (in press).
- ¹³ Property of reactor core (in Japanese) (Nihon Cut Core Trans co., Ltd.) www.nihon-cutcore.co.jp/file/standard_core.pdf.